AIAA 80-1408R

Reattachment of a Compressible Turbulent Free Shear Layer

G.S. Settles,* D.R. Williams,† B.K. Baca,‡ and S.M. Bogdonoff§
Princeton University, Princeton, N.J.

An experimental study is described in which a two-dimensional free turbulent shear layer at Mach 2.92 and a high Reynolds number is reattached to an inclined surface. The test geometry is designed specifically to create an undisturbed free shear layer which forms a well-defined initial condition for the reattachment process. Detailed flowfield surveys were made with mean pressure probes and the hot-wire anemometer. The results indicate that the free shear layer reached an equilibrium condition in terms of mean profile similarity, and support previous conclusions that flow reattachment may be correlated in terms of the free interaction concept. The redeveloping turbulent boundary layer downstream of reattachment shows an extremely rapid recovery which seems to proceed along a path of local equilibrium.

Nomenclature

c_f = skin friction coefficient
e' = voltage fluctuation
$\bar{E}$ = mean hot-wire anemometer bridge voltage
H = boundary layer shape parameter, $\equiv \delta^*/\theta$
L = length along shear layer from virtual origin, cm
M = Mach number
p = pressure, N/m^2
Re_∞ = freestream unit Reynolds number, m^{-1}; $\equiv u_\infty/\nu_\infty$
R_w = wire resistance, ohms
S_u = hot-wire sensitivity to velocity
S_ρ = hot-wire sensitivity to density
S_{T_t} = hot-wire sensitivity to stagnation temperature
$S_{\rho u}$ = hot-wire sensitivity to mass flux, $\equiv \partial \ell n \bar{E}/\partial \ell n \rho u$
T = temperature, K
u, U = velocity in x direction, m/s
u^* = Van Driest generalized velocity, m/s
u = friction velocity, m/s
W = wake function after Coles, $\cong 1-\cos(\pi y/\delta)$
x, X = distance along model surface in cm measured from reference point 5.08 cm upstream of separation lip; also measured from leading edge of reattachment ramp
y, Y = height above and normal to model surface, cm
β_k = equilibrium pressure gradient parameter, $\equiv (\delta^*_k/\tau_w)(\partial p/\partial x)$
δ = boundary-layer thickness, cm
δ^* = boundary layer displacement thickness, cm; $\equiv \int_0^\delta (1-\rho u/\rho_e u_e)\,dy$
δ_k^* = boundary layer kinematic thickness, cm; $\equiv \int_0^\delta (1-u/u_e)\,dy$
η = shear layer similarity parameter, $\equiv \sigma(Yu_e/2-Y)/L$
θ = boundary-layer momentum thickness, cm; $\equiv \int_0^\delta (\rho u/\rho_e u_e)(1-u/u_e)\,dy$
λ = incoming shear layer width, and interaction scaling parameter, $\equiv 2L/\sigma$
ν = kinematic viscosity, m^2/s
Π = boundary-layer wake-strength parameter
ρ = density, kg/m^3
σ = free shear layer spreading rate parameter, $\equiv L/(Yu_e/2-Y_{0.95u_e})$
τ_w = wall shear stress, N/m^2
τ_{wr} = hot-wire overheat ratio, $\equiv (T_w-T_r)/T_r$
$\langle\ \rangle$ = rms value

Subscripts

C = cavity
div = dividing streamline
e = local shear-layer edge value
F = final
k_1 = critical point after reattachment
ℓ, L = local
r = recovery
R = reattachment
t = stagnation conditions
w = wall; also wire
0 = incoming or undisturbed condition
∞ = incoming freestream value

Superscripts

$(\ )'$ = fluctuation
$(\bar{\ })$ = mean value

Introduction

AFTER decades of intensive study, the elusive problems of flow separation remain at the forefront of research in fluid mechanics. The practical examples, often compressible and almost always turbulent, are also the most difficult ones to understand. While slow progress is being made through cooperative experiments and computations, much still remains to be done.

In compressible flow interactions, the phenomena of boundary-layer separation and subsequent reattachment often are connected intimately in complex flow geometries. Some understanding has been gained in attempts, beginning with Ref. 1, to study separation by itself in experiments where it is independent of downstream conditions. The time-honored "free interaction" concept grew out of this approach.

Similar attempts to scrutinize flow reattachment have been fewer and less successful, partly because of the difficulty of experimentally isolating the reattachment process. Much of the experimental documentation of reattachment comes from studies of flow over a backstep,[2-4] which is of practical im-

Presented as Paper 80-1408 at the AIAA 13th Fluid and Plasma Dynamics Conference, Snowmass, Colo., July 14-16, 1980; submitted Sept. 19, 1980; revision received May 21, 1981.

*Professional Research Staff Member and Lecturer, Mechanical and Aerospace Engineering. Member AIAA.
†Graduate Research Assistant.
‡Graduate Research Assistant. Now with Sandia Corp., Albuquerque, N. Mex.
§Professor and Chairman, Mechanical and Aerospace Engineering. Fellow AIAA.

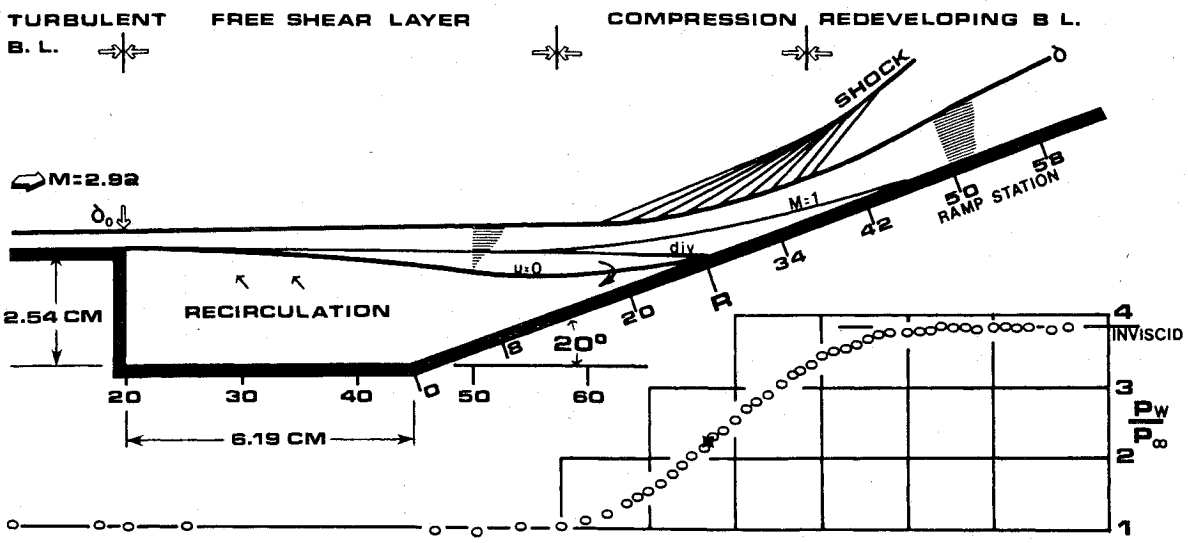

Fig. 1 Experimental model of the reattachment interaction with wall pressure distribution.

portance and is convenient for wind-tunnel studies. Unfortunately, a simple backstep is not the best geometry with which to study compressible flow reattachment because the resulting flow expansion and lip shock cause varying effects on the developing free shear layer, and thus confuse the initial conditions for reattachment. The reason for the present research is to study the reattachment process in an experiment tailored especially to eliminate those disadvantages.

This research grew out of an earlier exploratory study[5] in which a large, constant-pressure axisymmetric separated region was created. This allowed the development of a shear layer which was free of the effects of an expansion or lip shock, so that the reattachment of the layer could be studied with well-defined upstream conditions. The present, two-dimensional version of this test geometry is one which has been used successfully by other investigators,[6] but mainly to study the free shear layer only. The scope of the present work includes the reattachment process and the downstream boundary-layer redevelopment as well.

In this study, an equilibrium turbulent boundary layer was developed on a flat plate. The layer then separated at a sharp lip, forming a free shear layer that bridged a cavity to reattach upon a movable ramp. The ramp was adjusted so that the shear layer came straight off the plate with no wave disturbance and no pressure change up to the beginning of the reattachment compression.

The mean flow developed over this test geometry was surveyed in detail. Some preliminary fluctuation measurements were also carried out using hot-wire anemometry with appropriate modifications for supersonic flow. This data set was then analyzed and compared with a number of experiments and correlation schemes which are available in the literature.

The general framework for the present mean-flow analysis is the Van Driest compressibility transformation[7] coupled with the Coles wall-wake law.[8] Together, these concepts provide a powerful means of correlating Mach and Reynolds number effects in the experimental data, thus making it easier to distinguish the effect of a pressure gradient or of other parameters.

The overall goal of this work is to learn more about the physics of the compressible shear layer reattachment and redevelopment process. A second goal is to provide a detailed test case for the available prediction techniques, which include the flow models of Chapman-Korst[1,9] and Lees-Reeves,[10] and the computational solutions of the time-averaged Navier-Stokes equations with turbulence modeling.[11,12] Tabulations of the present data are available for this purpose,[13] and more detail on the experiment is given in Ref. 14.

Experimental Techniques

Wind Tunnel and Test Conditions

These experiments were carried out in the Princeton University 20×20-cm high Reynolds number supersonic wind tunnel at a freestream Mach number of 2.92±0.01. The stagnation pressure of 0.69 MN/m^2 ±0.5% and the stagnation temperature of 258 K±4% yielded a freestream unit Reynolds number of 6.7×10^7/m±3%. The freestream turbulence level was between 1 and 2% [expressed in terms of $\langle(\rho u)'\rangle/\rho_\infty u_\infty$].

Test Model

An elevation view of the test model and flowfield is given in Fig. 1. A turbulent boundary layer developed initially on a flat plate of 22.9-cm length, then separated over a sharp backward-facing step. The resulting free shear layer bridged a cavity of 2.54-cm depth and reattached on a plane ramp, 16-cm long and inclined 20 deg to the horizontal. The movable ramp was adjusted so that there was essentially no change in pressure or flow direction when the boundary layer separated. (The ratio of plate pressure to cavity pressure was monitored to insure this condition; its average value over the test series was 1.04.)

The cavity and ramp did not span the entire 20.3-cm width of the test model, but were inset by 2.54 cm on each side. This was done to avoid interference from the wind-tunnel sidewall boundary layers. Aerodynamic fences attached to both sides of the ramp were also used to help provide two dimensionality.

The ramp, cavity, and plate were heavily instrumented with 0.54-mm-diam surface pressure taps and a few surface thermocouples. Readings from the latter confirmed that the model surface was essentially adiabatic ($T_w/T_{t_\infty}\simeq1.03$).

Flowfield surveys were carried out in a vertical streamwise plane that was offset by 1.59 cm from the model centerline in order to avoid the main row of surface taps. For convenience in later figures, the streamwise survey locations are identified mainly by station numbers (STA), wherein stations along the plate and free shear layer begin at a point 5.08 cm ahead of the separation lip, while stations on the ramp begin at its leading edge at the cavity floor. The station numbers are numerically equal to 3.94 times x in cm (10.0 times x in inches).

Mean Flow Measurements

A traversing mechanism in the wind-tunnel ceiling was used to insert streamlined probes into the flow from above and downstream. These probes were designed specifically to avoid

any significant wave interference at or upstream of the reattachment line.

The pitot pressure was sampled by a flattened probe tip which was 0.18-mm high and 0.84-mm wide. The static pressure probe was a cone-cylinder type made of 0.81-mm-diam hypodermic tubing with two sampling holes located 10 diam downstream of the cone-cylinder junction and oriented in a vertical plane.

Hot-Wire Measurements

In order to measure some fluctuating properties of the turbulent flow, a DISA 55M10 constant-temperature hot-wire anemometer with 5-μm-diam tungsten wires was used. Several wires were required, all with length-to-diameter ratios of about 200. The wires were protected from the tunnel starting shock by a shield mounted on the supporting fin of the probe drive mechanism.

It is well known that the hot-wire voltage fluctuations are related to flow parameters by the equation

$$\frac{e'}{\bar{E}} = S_\rho \frac{\rho'}{\bar{\rho}} + S_u \frac{u'}{\bar{u}} - S_{T_t} \frac{T_t'}{\bar{T}_t} \tag{1}$$

Horstman and Rose[15] have shown that, when the wire Reynolds number is greater than 20 and the overheat ratio τ_{wr} is greater than 0.5, then $S_\rho = S_u = S_{\rho u}$ and Eq. (1) reduces to

$$\frac{e'}{\bar{E}} = S_{\rho u} \frac{(\rho u)'}{\overline{\rho u}} - S_{T_t} \frac{T_t'}{\bar{T}_t} \tag{2}$$

Further, when the hot wire is operated at high overheat ratios, the temperature sensitivity is smaller than the mass flow sensitivity. Coupling this with the assumption of a low level of temperature fluctuations leads to the following simplified relation:

$$\frac{e'}{\bar{E}} = S_{\rho u} \frac{(\rho u)'}{\overline{\rho u}} \tag{3}$$

which was used in evaluating the data.

Each wire was calibrated for temperature and mass flow sensitivities in a small pilot version of the 20×20-cm tunnel. The mass flow sensitivity was obtained by varying the freestream mass flow rate from 50-1000 kg/(m^2-s^2). The temperature sensitivity was obtained indirectly by repeating the mass flow calibration for five different overheat ratios (obtained by changing the hot-wire bridge resistance rather than the stagnation temperature). The response of the hot wire as a function of overheat ratio at constant mass flow rate was found from each mass flow calibration. Then the temperature sensitivity could be determined from $\partial \ln \bar{E} / \partial \ln R_w$ and other anemometer parameters.

We found that the temperature sensitivity is smaller than the mass flow sensitivity when the overheat ratio is greater than 1.0. So, to insure that the hot-wire response was primarily a function of mass flow, τ_{wr} was maintained between 1.0 and 1.3 for the present measurements.

The combination of very high Reynolds number and high turbulence intensity proved to be a harsh environment for the hot-wire probe (perhaps as harsh as any yet encountered in supersonic testing). Many wires were lost before a sufficiently rugged construction technique was evolved. The technique that worked best involved welding the 5-μm tungsten wires to the stainless steel support prongs using a tungsten electrode and a carefully-controlled capacitor discharge. Some slack was given to the wire to avoid strain-gaging, and rubber cement "shock absorbers" were applied to the welds. Wires installed in this manner survived a number of surveys in the reattachment flowfield before breakage occurred.

Data Acquisition and Reduction

The mean pitot and static pressure surveys, along with the essentially constant total temperature, were reduced in the traditional manner to yield profiles of Mach number, density, mean streamwise velocity, and related quantities. The compressible wall-wake law[7,8] was fitted to the resulting velocity profiles by a least-squares computer code, yielding values of c_f, δ, and Π. Following appropriate filtering, the fluctuating component of the hot-wire signal was digitized directly at a 500 kHz sampling rate through a Preston Scientific GMAD-1 A/D converter, and was then stored at high speed in the memory of a HP1000 minicomputer. Digital data analysis was then carried out using fast-Fourier-transform techniques.

Accuracy and Errors

The accuracies of the calibration standards used for pressures and temperatures were verified to be better than 1%. Complete calibrations were performed before each test series, and a calibration was repeated if a nonlinearity greater than 1% was found.

Several of the mean-flow profiles were repeated at least once as a consistency check. The static pressure probe response to pitch angle, known to be a potential problem, was measured carefully and minimized by choosing a vertical orientation of the sensing holes. Further, a series of tests was aimed at evaluating the effect of probe interference on the sensitive balance between the plate and cavity pressures.

These interference tests showed no effect of probing downstream of reattachment and little effect of probing near reattachment or above the zero velocity line of the free shear layer. Unfortunately, the presence of probes within the reversed-flow region led to discrepancies in the pressure balance of about 10%, which were considered unacceptable. Plans to survey this region with the current instrumentation setup were then abandoned.

Sensitivity tests in the data reduction showed that the error introduced by assuming a constant total temperature (instead of a measured profile) was only 0.5%. Similar tests indicated a 1-2% possible error involved in the minor corrections which were necessary to reconcile the static pressure profiles with the wall and freestream boundary conditions. A single example (station 54) showed that the error in measured pitot pressure due to velocity fluctuations was less than +2% across the profile.

The measurements are least trustworthy in the immediate vicinity of flow reattachment, due to the combined effects of probe interference and the unknown effective pitch angle of the static pressure probe. The latter error appears to dominate all others, since it could conceivably reach ±10%. Elsewhere in the flowfield the authors trust the static pressure measurements within ±4%. The pitot pressure measurements, being much less sensitive to pitch, are trusted within ±2%. The data reduction process tends to suppress some of these uncertainties and to add others. Following the method of Kline and McClintock, the mean Mach number and velocity are assigned uncertainties of, at worst, ±3% and ±5%, respectively, and are believed to be better than this everywhere except in the immediate vicinity of flow reattachment.

The hot-wire anemometer measurements are preliminary, since they are the first we have made in such a harsh flow environment. It is difficult to assign an uncertainty at this time, but hot-wire data are known to have a large susceptibility to error where fluctuations of up to 50% are indicated. The hot-wire results presented here are not meant to give the impression of great accuracy, but clearly they do capture the general characteristics and levels of the fluctuations. Recently, these hot-wire measurements have been repeated with more accuracy in experiments to be covered in a future publication.

Results and Discussion

Experimental Flowfield Map

A scaled map of the flowfield features is provided in Fig. 1. The measured wall pressure distribution is also shown.

The incoming turbulent boundary layer separates without turning, forming a free shear layer. This layer spreads more rapidly into the cavity than into the outer, supersonic flow. The mean dividing streamline between the outer flow and the inner (recirculating) flow is substantially straight but not exactly parallel with the outer streamlines. Thus the reattachment line is observed to fall slightly below the geometric extension of the flat plate onto the ramp surface.

A distributed compression on the ramp reverses the bottom of the incoming shear layer while turning the outer flow through an angle of 20 deg. The zero velocity line in the cavity and the sonic line above it become curved through an interaction with this pressure gradient.

Downstream of reattachment a new boundary layer develops on the ramp through the relaxing adverse pressure gradient followed by a constant pressure region. The sonic line in this layer is gently curved, and remains at a substantial distance from the surface until about the end of the pressure gradient. The thickness of this turbulent boundary layer grows rapidly with distance downstream. The wall pressure increases in a regular fashion from its upstream value to the final, inviscid value dictated by the turning of the outer flow.

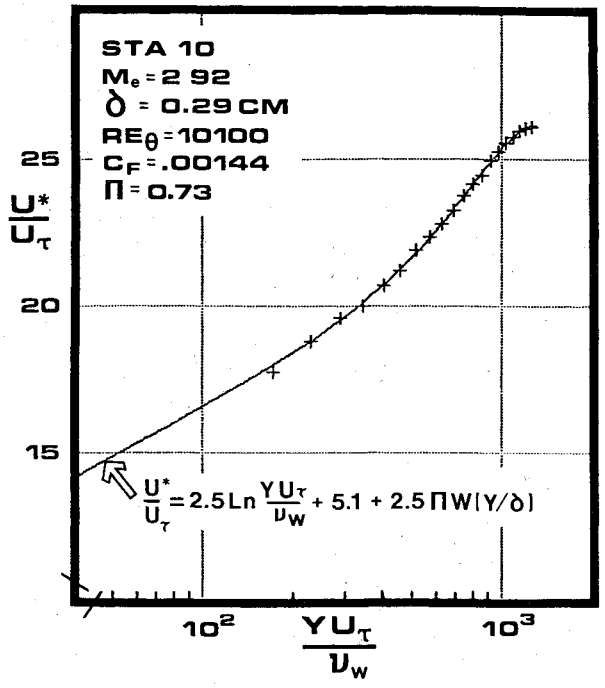

Fig. 2 Incoming turbulent boundary layer mean velocity profile in wall-wake coordinates.

Two-Dimensionality

It was expected that insuring two-dimensionality in this experiment would be difficult. Considering the large size and relatively small aspect ratio of the separated flow, the result was surprisingly good. As supported by the following evidence, the experiment met our standards for an essentially two-dimensional flow.

The spanwise surface pressure distribution, measured at several stations along the ramp, is constant and does not deteriorate downstream. The surface flow pattern indicates a straight reattachment line and no significant spanwise flow. (Other recent experiments by the authors[17] have demonstrated, though not for the first time, how sensitive the surface flow pattern is to a small lateral gradient.) The streamwise wall pressure distribution levels off at the expected inviscid value with no evidence of three-dimensionality. Finally, a spanwise Preston tube traverse just downstream of the reattachment line revealed a constant pressure independent of span.

Aerodynamic fences at the sides of the ramp were helpful in eliminating outflow and isolating the interaction from the wind-tunnel sidewall boundary layers. The parameters of the flowfield were not affected by changes in the fence size or location above the minimum size required to prevent leakage.

The current evidence on streamwise vortices after reattachment is contradictory. A weak indication of a cellular spanwise structure[18] was noticed in the surface flow patterns, but not in any other measured quantity. Such evidence was noticeably absent from the spanwise Preston tube reading.

Flowfield Steadiness

A series of microsecond spark shadowgrams revealed that the only detectable unsteadiness in the flowfield is that of the turbulent eddies and a slight "tremble" of the wave system, that is presumed to result from eddy motion above the sonic line. The scale of this wave motion is the same as in similar past studies,[19,20] namely, a small fraction of the average shear layer thickness. Such motion is not considered significant, so the mean flowfield is clearly defined. Note that a similar

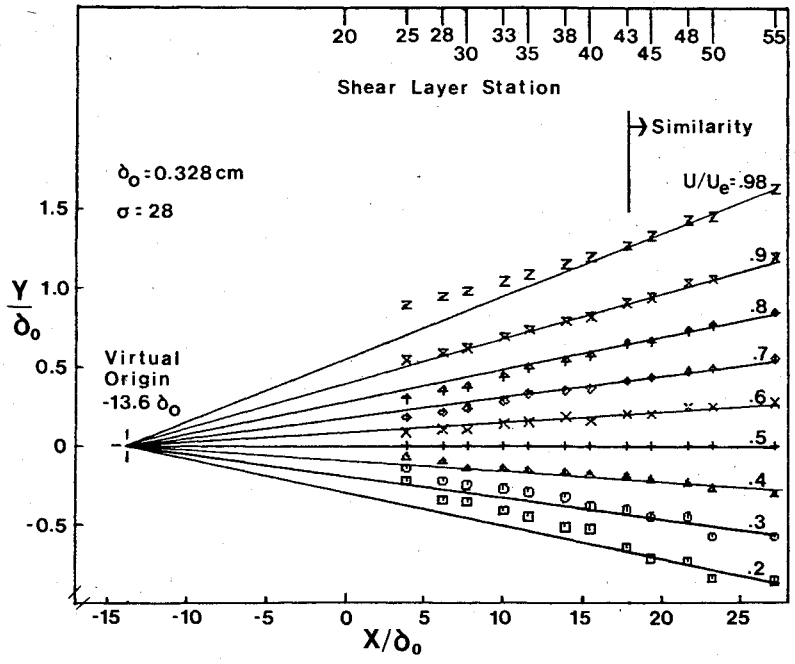

Fig. 3 Lines of constant velocity in the free shear layer, showing constant growth rate and virtual origin.

conclusion does not necessarily hold in low-speed flows, where the motion of the reattachment line after a backstep has been observed to be in the range of one step height.[21]

Upstream Flat-Plate Boundary Layer

An equilibrium flat-plate boundary layer forms the initial condition for the free shear layer in this experiment. Natural transition occurs within 3 cm of the plate leading edge at the present high Reynolds number, so no tripping devices are necessary or desirable. The turbulent boundary-layer profile approaching the separation lip is shown in wall-wake coordinates in Fig. 2. Its skin friction coefficient and wake-strength parameter are both close to the expected values for an equilibrium, zero-pressure-gradient boundary layer at this Reynolds number (0.00153 and 0.62, respectively).

The measured rms mass flow fluctuation level in the present flat-plate boundary layer reaches a maximum of about 8%. The profile of these fluctuations is in agreement with the range of similar measurements cited in the literature for equilibrium compressible turbulent boundary layers.[22]

Free Shear Layer

Mean-Flow Growth and Similarity

The free shear layer develops at constant pressure from the initial turbulent boundary layer. The conditions for similarity are simpler in the free shear layer than in the boundary layer due to the removal of the viscous constraint at the wall. Once the viscous scaling disappears, the only remaining scaling parameters are velocity and length, hence the common observation that free turbulent flows achieve similarity in normalized physical coordinates (as in laminar flow).

Such scaling is shown for the present free shear layer in Fig. 3, where lines of constant velocity are plotted vs streamwise distance. A development region and an eventual linear growth rate are observed. A distance of roughly 18 initial boundary-layer thicknesses downstream of separation is required to achieve this linear growth. Other investigators[5,6,23] have found this length to be as small as $10\delta_0$ and as large as $22\delta_0$, partly due to the obvious difficulty in defining it precisely.

The effect of the finite initial boundary layer can be accounted for[6] by finding the common virtual origin of the constant velocity lines in the linear growth region. From Fig. 3, the virtual origin of the present shear layer lies at about $14\delta_0$ ahead of separation. Knowing this length and the shear layer spreading rate parameter σ, the developed shear layer can be treated as if it had grown from a condition of no initial boundary-layer thickness.

The shear layer spreading parameter derived from Fig. 3 is $\sigma = 28$. This value agrees with the recently-established experimental trend in compressible free turbulent shear flow: that there is a definite effect of rising Mach number which decreases the shear layer growth rate. Bradshaw[24] points out that this is a real failure of Morkovin's hypothesis (that density fluctuations are not important in supersonic turbulence), since the same effect cannot be found by simply varying the density ratio in a low-speed flow.[25]

Further evidence of mean-flow similarity in the present free turbulent shear layer is shown in Fig. 4, where the mean velocity profiles in the fully-developed region (stations 43-55) are plotted on similarity coordinates. Coles' wake function, when plotted in the form of

$$u/u_e = \tfrac{1}{2} W[(\eta+1)/2] \tag{4}$$

is in excellent agreement with these measurements.

Turbulent Fluctuation Measurements

Despite the evidence noted for a fully-developed free shear layer based on mean-flow similarity, there is still a question regarding the turbulent fluctuations. Nine shear layer stations were surveyed by the hot-wire anemometer to address this question. The results show that the fluctuation intensity,

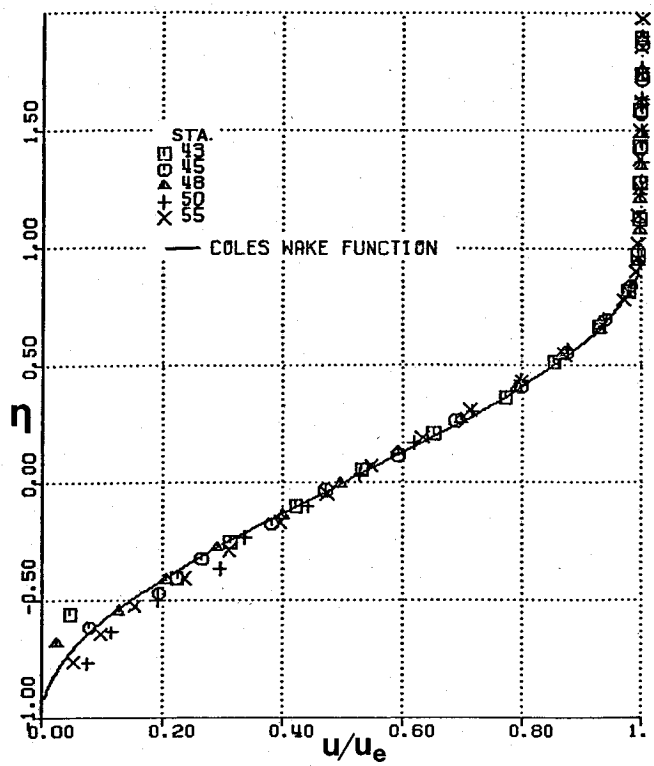

Fig. 4 Similarity plot of free shear layer velocity profiles, compared with Coles' wake function.

normalized by the local mean value, increases with distance along the shear layer, and that similarity of these fluctuation profiles is not achieved even where the mean profiles are similar. However, considering that the shear layer has reached an asymptotic spreading rate in agreement with other experiments, the lack of a clear indication of equilibrium in these preliminary fluctuation measurements is believed to be of secondary importance.

The increase of fluctuation intensity with streamwise distance in a free shear layer has been noted by others in both low- and high-speed experiments.[21,26] It is thought by some[21,27] to result from the feedback of turbulence energy produced near reattachment and convected back into the shear layer by the recirculating flow. Another plausible explanation might be that the inflected mean velocity profile of the shear layer feeds mean-flow energy into turbulence production. In any case the production or convection of turbulence is expected to equilibrate eventually with the diffusion, dissipation, and pressure destruction terms if the shear layer is long enough, thus leading to some sort of similarity of turbulence profiles.

Kim et al.[24] found that the location of the maximum turbulence intensity in their low-speed free shear layer coincided with the dividing streamline. That conclusion appears to be roughly correct for the present measurements as well.

Reattachment Region

One goal of the present study is to provide a further check on existing correlations and analyses of the flow reattachment process. The Chapman-Korst flow model[1,9] is a classic example of the latter, that involves a number of assumptions that are more or less confirmed by experience. One of the weakest of these assumptions proposes that reattachment occurs at the end of the pressure gradient, which does not agree with any of the past or present results (see Fig. 1). A simple correction, proposed by Nash,[28] locates the reattachment point on the pressure rise by the following formula.

$$(p_R - p_C)/(p_F - p_C) = 0.35 \tag{5}$$

The left-hand side of Eq. (5) evaluated from present results is 0.38, which generally supports Nash's correction.

A more sophisticated, though still empirical modification of the Chapman-Korst model was proposed by Sirieix et al.,[29,30] following their extensive set of measurements. One of the key assumptions in the Sirieix model proposes that the thickness of the turbulent layer is a minimum above the "critical point" after reattachment, which is confirmed by the present results.

Another successful feature of the Sirieix model is the removal of the initial boundary-layer influence on reattachment by way of the virtual origin of the shear layer. Sirieix et al.[30] used the same test geometry and Mach number as the present study to develop a correlation for the initial boundary-layer effect on the reattachment angle. The present result is in very good agreement with their correlation and data.

Free Interaction Scaling

A free interaction, as defined by Chapman et al.,[1] is an interaction which depends upon incoming flow conditions but not upon conditions downstream. Boundary-layer separation in supersonic flow is known from experience to behave in this manner if downstream disturbances do not occur too close to the separation point. A critical point after separation begins the region wherein disturbances do not propagate upstream.

Sirieix et al.,[29] have attempted to apply this principle to flow reattachment as well. Their critical point falls just downstream of the reattachment line (at about station 33 on the ramp in the present experiment). Using the incoming shear layer thickness λ as a scaling parameter, Sirieix et al. were able to collapse their own measurements of reattachment wall pressure distributions onto a single similarity curve, which is reproduced here in Fig. 5. Their measurements were carried out over a range of Mach numbers with various geometry changes downstream of the critical point to demonstrate the absence of upstream propagation.

The present wall pressure distribution agrees with the correlation in Fig. 5, which lends further support to the claim of Sirieix et al. that reattachment can be described in free interaction terms. It follows that λ is the proper scaling length for the reattachment process rather than a step height or boundary-layer thickness somewhere upstream. Further, the boundary-layer redevelopment downstream of the critical point is "disconnected" from reattachment and the shear layer upstream, at least insofar as upstream propagation of disturbances is concerned.

These are strong conclusions to be drawn from a simple collapse of wall pressure data. One must bear in mind that the coordinates of Fig. 5 force a fit at the upstream condition and at the critical point, so only a difference in the normalized value of $\partial p/\partial x$ will be apparent. On the other hand, other investigators[3,5] have observed the similarity of reattachment pressure distributions in other coordinate systems, and many other investigators have observed the lack of effect of downstream disturbances on reattachment (e.g., Refs. 3 and 31).

Batham,[32] assuming that reattachment is a free interaction, has used the momentum equation (with some assumptions) to arrive at an empirical correlation of the reattachment pressure coefficient and the edge Mach number. His correlation works well for a number of published experiments including the present one. To the authors' knowledge, there is no evidence against the validity of the free interaction concept for flow reattachment.

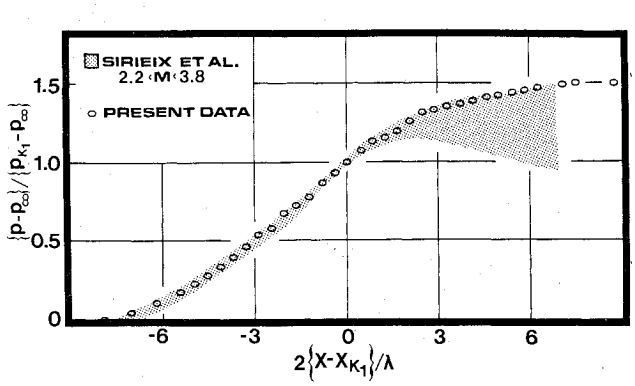

Fig. 5 Free interaction correlation of reattachment wall pressure distributions for various Mach numbers and geometries, including present data.

Boundary-Layer Redevelopment

The turbulent boundary layer which develops downstream of reattachment is subject to three coupled, nonlinear effects, namely, the restoration of the viscous constraint at the wall, a strong adverse pressure gradient, and a 20 deg change in streamline direction. How the boundary layer responds to these effects is discussed next on the basis of the present experimental results.

Static Pressure Variations

The pressure changes across the redeveloping boundary layer follow the waves of the distributed compression fan which turns the flow above the sonic line. There is a definite normal pressure gradient, $\partial p/\partial y$, across the boundary layer, which weakens in the downstream direction. At reattachment there is a 25% drop in static pressure from the wall to the boundary-layer edge. This drop decreases to only 1.5% at station 61, the last survey location on the ramp. Chow and Spring[33] have interpreted this relaxation of $\partial p/\partial y$ as the main process in the redevelopment of the boundary layer.

Mean Velocity Profiles

The mean streamwise velocity profiles of the redeveloping boundary layer downstream of reattachment are shown in Fig. 6 in y/δ vs u/u_e coordinates. There is a very rapid "filling out" of the profiles in the short distance from reattachment to the last survey station. While the profile at reattachment is almost a pure wake (as is the incoming shear layer), the last few profiles have a velocity ratio greater than 0.8 at only one-tenth of δ away from the wall. This rapid development is reminiscent of published results for "wall jets."

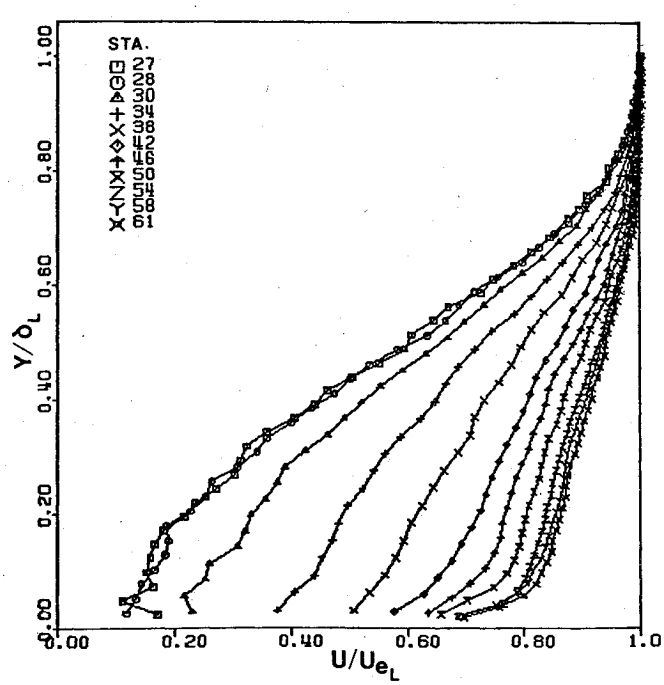

Fig. 6 The redevelopment of normalized mean velocity profiles in the boundary layer downstream of reattachment.

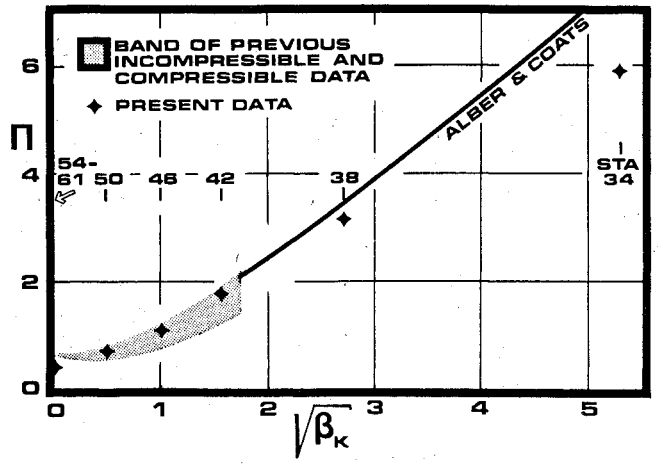

Fig. 7 Wake-strength parameter vs equilibrium pressure gradient parameter in redeveloping boundary layer, compared with previous data.

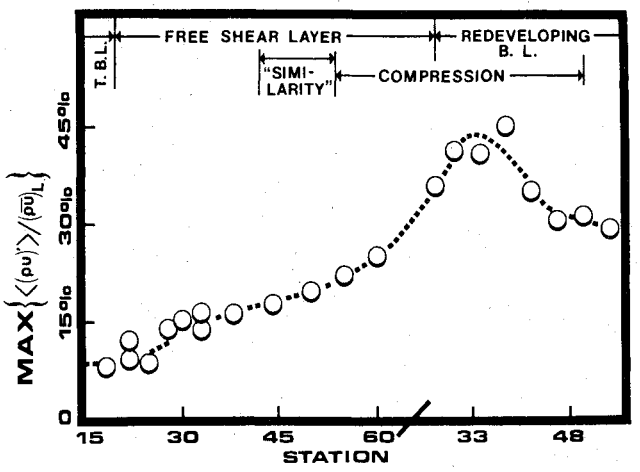

Fig. 8 Plot of local maximum rms mass flow fluctuations vs distance along the entire length of the interaction.

The explanation of this behavior is not obvious. It seems, based on qualitative flow visualization results, that the high velocity near the wall results from considerably enhanced turbulent mixing, perhaps due to the formation of large eddies. It would be interesting to follow this phenomenon further downstream if not for the limits of the experimental geometry. Bradshaw and Wong[34] did follow it further downstream in low-speed flow, and found that the wall-wake law was not strictly applicable within 30 incoming shear layer thicknesses after reattachment. Since the present ramp ends after a length of only about 7 incoming thicknesses, we conclude that we are observing only the initial part of the boundary-layer redevelopment process.

The profile shape parameters H and Π both show a considerable decrease as the redeveloping profile becomes "fuller." However, while H tends toward a constant value of 3, Π continues to decrease below the accepted flat-plate equilibrium value of 0.62. This conclusion holds even in view of the uncertainty in determining Π due to a poor fit with the wall-wake law downstream of station 42. It appears from a consideration of the low-speed results[34,35] that a much greater distance is required in the downstream direction before profile similarity is reached in terms of the wall-wake law.

Local Equilibrium

There is ample experimental and analytical background to support the hypothesis that "local" equilibrium can occur in turbulent boundary layers subjected to moderate pressure gradients.[36-38] Under local equilibrium the boundary layer is characterized by local conditions only, and maintains similarity for a given pressure gradient. One would then expect to be able to correlate some overall profile shape parameter with a suitable nondimensional pressure gradient parameter. Experience shows this to be the case for incompressible flows[36-38] and for some compressible flows as well,[16,39,40] when framed in equivalent incompressible terms.

For purposes of the present redeveloping boundary layer, the wake-strength parameter is examined as a function of the local pressure gradient in Fig. 7. Following the experience of Lewis et al.,[16] the Clauser pressure gradient parameter is freed of Mach number dependence by defining it in terms of the kinematic thickness δ_k^*, rather than the compressible displacement thickness δ^*. The available low- and high-speed results are indicated in Fig. 7 along with the present measurements.

The surprising result of this correlation is that the redeveloping boundary layer in the present experiment relaxes along the previously established local equilibrium curve. This is surprising in that it was not expected that a boundary layer that is developing so rapidly would be near any sort of equilibrium. It would be unwise to draw strong conclusions from the sparse supportive measurements shown in Fig. 7. However, such a rapid establishment of local equilibrium as is suggested by this result would be a powerful concept if it could be eventually supported by a range of careful experiments.

Turbulent Fluctuations

The evolution of local maximum mass flow fluctuations throughout the present flowfield is plotted in Fig. 8. A gradual rise in fluctuation intensity is observed from the initial boundary layer along the free shear layer. A peak of the maximum mass flow fluctuations occurs at about the middle of the compression region, followed by a fairly rapid decay further downstream. The highest fluctuation level observed in the flowfield, about 40-50%, is in agreement with other similar measurements.[41-43] Further, the 30% maximum fluctuation level in the last profile obtained is far above the expected level in an equilibrium flat-plate, turbulent boundary layer.[22]

Summary and Conclusions

A detailed experimental documentation is given of the reattachment and redevelopment of a free turbulent shear layer in two-dimensional compressible flow. The experiment was carried out under adiabatic conditions at Mach 2.92 with a freestream Reynolds number of 6.7×10^7/m. The test model was especially designed to generate a disturbance-free, constant pressure shear layer in order to insure a well-defined initial condition for the reattachment process. Hot-wire anemometry was used with appropriate modifications to improve signal interpretation and wire survival in a harsh testing environment. Mean- and fluctuating-flow measurements were taken at a number of stations throughout the flowfield. The results are used to study the physics of the reattachment and boundary-layer redevelopment phenomena, and to provide a test case for numerical code validation. Several conclusions and observations have been found, as listed below.

1) Mean-flow similarity and a constant growth rate are achieved in the free turbulent shear layer within a distance of about 18 initial boundary layer thicknesses after separation. While preliminary hot-wire measurements show an increasing fluctuation level even beyond this point, a firm conclusion on the fluctuating state of the shear layer awaits the analysis of more rigorous hot-wire measurements now in progress.

2) Present results agree with those of previous investigators in that the flow up to the experimental critical point after

reattachment is a free interaction in the classical sense. Thus, simple empirical correlations for the surface pressure distribution and other flowfield features are successful in correlating the present results with those of others.

3) The mean-velocity profiles of the redeveloping boundary layer show a very rapid filling-out which is reminiscent of wall jet results, even though the length available for observing the redevelopment process is relatively short.

4) The conventional flat-plate equilibrium condition is not achieved within the limits of the measured redeveloping boundary layer, although the redevelopment process appears to proceed along the previously established path of local equilibrium with the imposed pressure gradient.

5) Measured turbulent fluctuation levels reach a maximum of 40-50% in the compression region near flow reattachment, then fall off rapidly in the redeveloping boundary layer downstream.

Acknowledgments

This work was supported by the U.S. Air Force Office of Scientific Research, Contract F44620-75-C-0080, monitored by Dr. James D. Wilson.

References

[1] Chapman, D.R., Kuehn, D.M., and Larson, H.K., "Investigation of Separated Flows in Subsonic and Supersonic Streams with Emphasis on the Effects of Transition," NACA Rept. 1356, 1958.

[2] Hastings, R.C., "Turbulent Flow Past Two-Dimensional Bases in Supersonic Streams," British Aeronautical Research Council R&M 3401, Dec. 1963.

[3] Roshko, A. and Thomke, G.J., "Observations of Turbulent Reattachment Behind an Axisymmetric Downstream-Facing Step in Supersonic Flow," *AIAA Journal,* Vol. 4, June 1966, pp. 975-980.

[4] Reda, D.C. and Page, R.H., "Supersonic Turbulent Flow Reattachment Downstream of a Two-Dimensional Backstep," AIAA Paper 70-108, Jan. 1970.

[5] Simpers, G., Vas, I.E., and Bogdonoff, S.M., "Turbulent Shear Layer Reattachment at M ~ 3," AIAA Paper 77-43, Jan. 1977.

[6] Sirieix, M. and Solignac, J.L., "Contribution a l'Etude Expérimentale de la Couche de Mélange Turbulent Isobare d'un Ecoulement Supersonique," French ONERA T.P. 327, 1966.

[7] Van Driest, E.R., "Turbulent Boundary Layer in Compressible Fluids," *Journal of the Aeronautical Sciences,* Vol. 18, March 1951, pp. 145-160.

[8] Coles, D., "The Young Person's Guide to the Data," *Proceedings of the 1968 AFOSR-IFP-Stanford Conference on Computation of Turbulent Boundary Layers,* Vol. 2, Stanford Univ., 1969, pp. 1-45.

[9] Korst, H.H., "A Theory for Base Pressures in Transonic and Supersonic Flow," *Journal of Applied Mechanics,* Vol. 23, Dec. 1956, pp. 593-600.

[10] Lees, L. and Reeves, B.L., "Supersonic Separated and Reattaching Laminar Flows: I. General Theory and Application to Adiabatic Boundary-Layer/Shock-Wave Interactions," *AIAA Journal,* Vol. 2, Nov. 1964, pp. 1907-1920.

[11] Rubesin, M.W., "Developments in the Computation of Turbulent Boundary Layers," *Turbulent Boundary Layers—Experiment, Theory, and Modeling,* Paper 11, NATO AGARD CP-271, 1979.

[12] Horstman, C.C., Settles, G.S., Williams, D.R., and Bogdonoff, S.M., "A Reattaching Free Shear Layer in Compressible Turbulent Flow—A Comparison of Numerical and Experimental Results," AIAA Paper 81-0333, Jan. 1981.

[13] Data Library, 1980-81 AFOSR-HTTM-Stanford Conf. on Complex Turbulent Flows, computer tape available from COSMIC, 112 Barrow Hall, Univ. of Georgia, Athens, Ga.

[14] Settles, G.S., Baca, B.K., Williams, D.R., and Bogdonoff, S.M., "A Study of Reattachment of a Free Shear Layer in Compressible Turbulent Flow," AIAA Paper 80-1408, July 1980.

[15] Horstman, C.C. and Rose, W.C., "Hot-Wire Anemometry in Transonic Flow," NASA TM X-62,495, Dec. 1975.

[16] Lewis, J.E., Gran, R.L., and Kubota, T., "An Experiment on the Adiabatic Compressible Turbulent Boundary Layer in Adverse and Favorable Pressure Gradients," *Journal of Fluid Mechanics,* Vol. 51, Pt. 4, 1972, pp. 657-672.

[17] Settles, G.S., Perkins, J.J., and Bogdonoff, S.M., "Investigation of Three-Dimensional Shock/Boundary Layer Interactions at Swept Compression Corners," *AIAA Journal,* Vol. 18, July 1980, pp. 779-785.

[18] Inger, G.R., "Three-Dimensional Heat- and Mass-Transfer Effects Across High-Speed Reattaching Flows," *AIAA Journal,* Vol. 15, March 1977, pp. 383-389.

[19] Behrens, W., "Separation of a Supersonic Turbulent Boundary Layer by a Forward-Facing Step," AIAA Paper 71-127, Jan. 1971.

[20] Settles, G.S., "An Experimental Study of Compressible Turbulent Boundary Layer Separation at High Reynolds Number," Ph.D. Dissertation, Aerospace and Mechanical Sciences Dept., Princeton Univ., Princeton, N.J., Sept. 1975.

[21] Kim, J., Kline, S.J., and Johnston, J.P., "Investigation of Separation and Reattachment of a Turbulent Shear Layer: Flow Over a Backward-Facing Step," Thermosciences Div., Stanford Univ., Stanford, Calif., Rept. MD-37, April 1978.

[22] Sandborn, V.A., "A Review of Turbulence Measurements in Compressible Flow," NASA TM X-62,337, March 1974.

[23] Ikawa, H. and Kubota, T., "Investigation of Supersonic Turbulent Mixing Layer with Zero Pressure Gradient," *AIAA Journal,* Vol. 13, May 1975, pp. 566-572.

[24] Bradshaw, P., "Compressible Turbulent Shear Layers," *Annual Review of Fluid Mechanics,* Vol. 9, 1977, pp. 33-54.

[25] Brown, G.L. and Roshko, A., "On Density Effects and Large Structure in Turbulent Mixing Layers," *Journal of Fluid Mechanics,* Vol. 64, Pt. 4, pp. 775-816.

[26] Wagner, R.D., "Mean Flow and Turbulence Measurements in a Mach 5 Free Shear Layer," NASA TND 7366, Dec. 1973.

[27] Bradshaw, P., "Turbulence Research—Progress and Problems," *Proceedings of the 1976 Heat Transfer and Fluid Mechanics Institute,* Stanford Univ. Press, Stanford, Calif., 1976, pp. 128-139.

[28] Nash, J.F., "An Analysis of Two-Dimensional Base Flow Including the Effect of the Approaching Boundary Layer," British Aeronautical Research Council R&M 3344, 1963.

[29] Sirieix, M., Mirande, J., and Délery, J., "Expériences Fondamentales sur le Recollement Turbulent d'un Jet Supersonique," NATO AGARD CP 4, Pt. 1, 1966, pp. 353-391; English translation in British RAE Library Trans. 1196, Nov. 1966.

[30] Sirieix, M., Délery, J., and Mirande, J., "Reserches Expérimentales Fondamentales sur les Ecoulements Séparés et Applications," French ONERA T.P. 520, 1967.

[31] Bogdonoff, S.M., Kepler, C.E., and Sanlorenzo, E., "A Study of Shock Wave Turbulent Boundary-Layer Interaction at Mach 3," PUAED Rept. 222, Princeton Univ., Princeton, N.J., July 1953.

[32] Batham, J.P., "A Reattachment Criterion for Turbulent Supersonic Separated Flows," *AIAA Journal,* Vol. 7, Jan. 1969, pp. 154-156.

[33] Chow, W.L. and Spring, D.J., "Viscous Interaction of Flow Redevelopment after Flow Reattachment with Supersonic External Streams," *AIAA Journal,* Vol. 13, Dec. 1975, pp. 1576-1584.

[34] Bradshaw, P. and Wong, F.Y.F., "The Reattachment and Relaxation of a Turbulent Shear Layer," *Journal of Fluid Mechanics,* Vol. 52, Pt. 1, 1972, pp. 113-135.

[35] Coles, D., "The Turbulent Boundary Layer in a Compressible Fluid," Rand Corp., Santa Monica, Calif., Rept. R-403-PR, 1962, App. A.

[36] Clauser, F.H., "Turbulent Boundary Layers in Adverse Pressure Gradients," *Journal of the Aeronautical Sciences,* Vol. 21, Feb. 1954, pp. 91-108.

[37] Coles, D., "Remarks on the Equilibrium Turbulent Boundary Layer," *Journal of the Aeronautical Sciences,* Vol. 24, July 1957, pp. 495-506.

[38] Mellor, G.L. and Gibson, D.M., "Equilibrium Turbulent Boundary Layers," *Journal of Fluid Mechanics,* Vol. 24, Pt. 2, 1966, pp. 225-253.

[39] Laderman, A.J., "Pressure Gradient Effects on Supersonic Boundary Layer Turbulence," Ford Aerospace and Communications Corp., Newport Beach, Calif., Rept. U-6427, Oct. 1978.

[40] Alber, I.E. and Coats, D.E., "Analytical Investigations of Equilibrium and Non-Equilibrium Compressible Turbulent Boundary Layers," AIAA Paper 69-689, June 1969.

[41] Rose, W.C. and Childs, M.E., "Reynolds-Stress Measurements in a Compressible Boundary Layer Within a Shock-Wave-Induced Adverse Pressure Gradient," *Journal of Fluid Mechanics,* Vol. 65, 1974, pp. 177-188.

[42] Gaviglio, J., Dussauge, J.-P., Debieve, J.-F., and Favre, A., "Behavior of a Turbulent Flow, Strongly Out of Equilibrium at Supersonic Speeds," *Physics of Fluids,* Vol. 20, Oct. 1977, pp. 5179-5192.

[43] Ardonceau, P., Lee, D.H., Alziary de Roquefort, T., and Goethals, R., "Turbulence Behavior in a Shock Wave/Boundary Layer Interaction," *Turbulent Boundary Layers—Experiment, Theory, and Modeling,* NATO AGARD CP-271, 1979.